

Synthesis and Properties of a Novel Superabsorbent Polymer Composite from Microwave Irradiated Waste Material Cultured *Auricularia auricula* and Poly (acrylic acid-co-acrylamide)

Zhiqiang Cheng,^{1,2} Junfeng Li,¹ Juntao Yan,¹ Lijuan Kang,² Xin Ru,¹ Mengzhu Liu¹

¹College of Chemistry, Jilin University, Changchun 130012, China

²College of Resource and Environmental Science, Jilin Agricultural University, Changchun 130118, China

Correspondence to: J. Li (E-mail: jfli@jlu.edu.cn)

ABSTRACT: A novel superabsorbent polymer composite was successfully synthesized from waste material cultured *Auricularia auricula* (WMCAA) and poly (acrylic acid-co-acrylamide) (P(AA-co-AM)) using microwave irradiation. Optimal synthesis conditions were determined by investigating the water absorbency of the superabsorbent composite. The effects associated with weight ratios of WMCAA, acrylamide (AM) monomers, initiators, and acrylic acid (AA) crosslinkers, as well as the degree of neutralization of AA were examined. The maximum water absorbencies were found to be 1548 g/g (distilled water) and 72 g/g (0.9% NaCl solution). Fourier transform infrared spectroscopy (FTIR) was applied to determine the molecular structure of the superabsorbent composite, and scanning electron microscopy (SEM) was used to demonstrate the characteristic compact and porous structure of the material. Further studies conducted via transmission electron microscopy (TEM) revealed the formation of a novel interpenetrating polymer network structure. Thermogravimetry/differential thermal (TG/DTG) analysis demonstrated improved thermal stability in the composite material compared with WMCAA. Additionally, high water absorption rates observed in the polymer during the swelling process indicated first-order kinetics. The water absorption and adsorption of the superabsorbent composite were studied in a variety of fertilizer solutions, revealing an indirect relationship between water absorbing ability and fertilizer concentration. Conversely, a direct relationship was observed between absorbed fertilizer and fertilizer concentration. © 2013 Wiley Periodicals, Inc. *J. Appl. Polym. Sci.* 130: 3674–3681, 2013

KEYWORDS: adsorption; bioengineering; biomedical applications

Received 24 April 2013; accepted 4 June 2013; Published online 26 June 2013

DOI: 10.1002/app.39621

INTRODUCTION

Superabsorbent polymers are characterized by the presence of a large number of strongly hydrophilic groups, an appropriate degree of crosslinking, and a three-dimensional (3D) network structure.^{1,2} These characteristics allow superabsorbent polymers to absorb more than one thousand times their own weight in water and to retain water even under elevated pressure conditions.^{3,4} Specific molecular groups can be grafted on the backbone of these polymers to produce tailored superabsorbent hydrogel materials with extensive commercial applications⁵ in hygienic products,⁶ agriculture,^{7,8} environmental protection,⁹ drug delivery,^{10,11} and bioengineering.¹²

Conventional synthetic methods for producing superabsorbent polymers are time-consuming and often require expensive specialized equipment to maintain necessary reaction conditions.^{13,14} Recently, new synthesis technologies utilizing high-efficiency superabsorbent resins have been developed that can save energy, while reducing pollution and costs involved in superabsorbent

material synthesis, such as microwave and ⁶⁰Co γ irradiation.^{15,16} As a relatively new synthetic polymer technology, irradiation effectively promotes chemical reactions under more favorable conditions than conventional methods. Using irradiation reaction times can be shortened, and efficiency can be improved.¹⁷ Additionally, no temperature gradient is required during the reaction, allowing synthesis to be substantially accelerated without O₂ or inhibitor removal.^{18,19} The environmental impact of irradiation technologies is also more manageable, applicable as pollutant-limiting dry-reaction or semidry reaction processes.²⁰

With over 400 million tons of mushrooms produced for both domestic use and export each year, China produces more commercial mushroom crops than any other country in the world.²¹ As a by-product of mushroom cultivation, waste material cultured *Auricularia auricula* (WMCAA) is an abundant bioresource. WMCAA primarily consists of mycelium (40–55%), crude protein (6–13%), crude fat (1–5%), and natural cellulose and hemicelluloses (10–30%).^{22,23} Although some WMCAA is

used in animal feed, organic fertilizer, and flower soil, most WMCAA is discarded or burned, a wasteful and polluting practice.^{24,25} Because of the abundance of WMCAA materials, effective, and comprehensive utilization of this bioresource should be carefully considered.

This study proposes a novel and economical superabsorbent polymer material based on acrylic acid (AA), acrylamide (AM), and WMCAA synthesized by microwave irradiation. Water absorption abilities, polymer network structure, and the P(AA-co-AM) matrix of the resultant superabsorbent composite WMCAA/P(AA-co-AM) were examined and characterized using transmission electron microscopy (TEM) and scanning electron microscopy (SEM). The resultant superabsorbent composites were characterized by Fourier transform infrared spectroscopy (FTIR), SEM energy dispersive spectroscopy (SEM-EDS), TEM, and thermogravimetry/differential thermal (TG/DTG). Furthermore, the water absorbencies of the resultant superabsorbent polymer materials were systematically investigated by examining the weight ratios of WMCAA, AM monomers, initiators, and AA crosslinkers, along with the degree of neutralization of AA, indicating optimal weight ratios and neutralization degrees for WMCAA, AMs, initiators, and AA crosslinkers.

MATERIAL AND METHODS

Acrylic acid (AA); analytical grade acrylamide (AM); *N,N*-methylenebisacrylamide (MBA); and potassium persulfate (KPS) were purchased from the Tianjin Reagent Corp (Tianjin, China). Analytical grade methanol and sodium hydroxide reagents were used, and all other reagents were prepared by distillation before use. Briefly, purity was ensured by distilling AA under reduced pressure and recrystallizing KPS from distilled water. WMCAA was acquired from the Bacteria Institute of Jilin Agricultural University (Jilin, China).

Preparation of the WMCAA/P(AA-co-AM) Superabsorbent Composite

WMCAA was crushed, ground in a colloid mill, and oven dried at 60°C for 2 h. A series of samples composed of variant amounts of WMCAA, MBA, and KPS combined with AA of variant neutralization degrees were prepared. Briefly, WMCAA was wetted using small volumes of distilled water and subjected to ultrasound pretreatment at 50°C for 5 min. Initiator (KPS), crosslinker (MBA), acrylamide (AM), and acrylic acid (AA) were added to the prepared WMCAA following gelatinization. The mixture was homogenized and allowed to undergo a controlled reaction for 5–8 min under 270 W microwave radiation. The resultant reddish-brown polymer was soaked in methanol for 4 h and dried to a constant weight in a vacuum oven at 50°C. Finally, the product was milled into 150–250 μm particles and stored for subsequent water absorption testing.

Water Absorbency Measurement

To determine water absorption capability, 0.100 g samples of superabsorbent composite were immersed in distilled water or 0.9% saline solution. The samples were allowed to swell until equilibrium at room temperature, and swollen samples were removed using a 150 μm filter screen. The water absorbency of

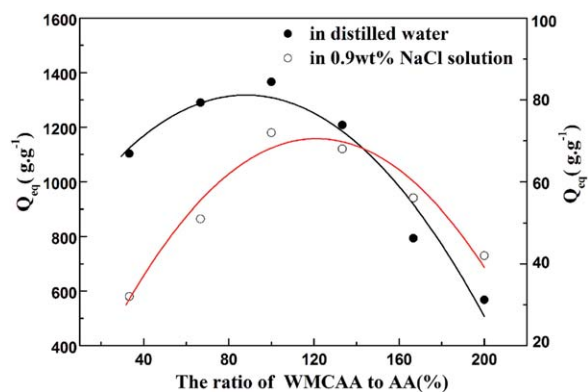


Figure 1. Effect of WMCAA to AA ratio on absorbencies. [Color figure can be viewed in the online issue, which is available at wileyonlinelibrary.com.]

the superabsorbent composite was determined by weighing the swollen sample and applying the following equation:

$$Q_{(\text{H}_2\text{O})} = \frac{m_2 - m_1}{m_1},$$

where m_1 is the weight of the dry superabsorbent polymer and m_2 is the weight of the swollen superabsorbent polymer. $Q_{\text{H}_2\text{O}}$ (g/g) expresses the swelling ratio of the material as grams of water per gram of sample (g/g).

FTIR Spectroscopy

A 10 mg sample of the superabsorbent composite material was prepared by grinding the sample with 300 mg of KBr for 20 min. The FTIR spectra of the resultant sample were obtained with a Nicolet 5PC FTIR spectrometer (ThermoScientific).

SEM-EDS and TEM Examination

Surface morphology of the superabsorbent composite was examined by SEM using an SSX-550 (Shimadzu, Japan). Samples were placed on aluminum stubs and coated with a thin layer of palladium gold alloy. EDS was completed using an SEDX-500 (Shimadzu, Japan) after coating samples with gold film. TEM data were obtained using a high-resolution JEM-1230 (JEOL, Japan) at an acceleration voltage of 100 kV. Notably, samples were ultrasonically dispersed in ethanol before observation.

Thermal Stability Characterization

TG/DTG analysis was performed using a Pyris 1TGA (Perkin Elmer) under a nitrogen atmosphere at a heating rate of 10°C/min. The temperature ranged from 30 to 800°C.

RESULTS AND DISCUSSION

Effect of WMCAA to AA Ratio on Absorbencies

The effect of the WMCAA to monomer (AA) weight ratio on absorbencies was studied, and results are shown in Figure 1. Superabsorbent composites absorbencies first increased and then decreased within increasing weight ratios of WMCAA to AA. This effect was apparent for samples submerged in distilled water or saline solution. At a ratio of 100 wt%, maximum absorbencies of 1366 g/g (distilled water) and 72 g/g (0.9 wt% NaCl solution) were observed.

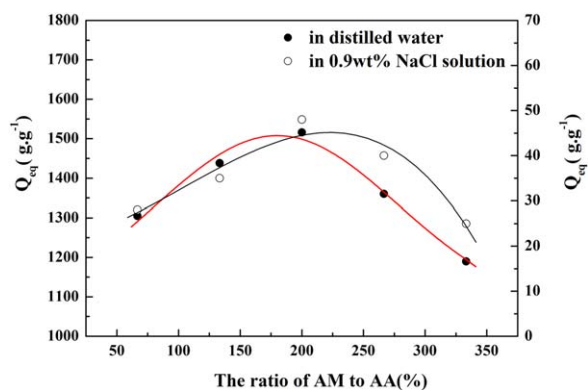


Figure 2. Effect of AM to AA ratio on absorbencies. [Color figure can be viewed in the online issue, which is available at wileyonlinelibrary.com.]

For ratios less than 100 wt%, absorbencies in distilled water increased with increasing WMCAA to AA weight ratios, likely caused by increased crosslinking between WMCAA and P(AA-co-AM) due to elevated WMCAA availability. Similarly, absorbencies in 0.9 wt% NaCl solutions increased with increasing WMCAA to AA weight ratios, likely due to the presence of large numbers of cations, such as NH_4^+ , Ca^{2+} , and Mg^{2+} , responsible for increasing osmotic pressure between the polymeric network and external solution.

Notably, for WMCAA to AA weight ratios exceeding 100 wt%, absorbencies in both distilled water and saline solution decreased with increasing WMCAA to AA weight ratio. This phenomenon may result a reduction in hydrophilic groups, such as $-\text{COOH}$, $-\text{COO}^-$, and $-\text{COONH}_2$, in the superabsorbent composite.

Effects of AM Content

AM content affected water absorbencies of the superabsorbent composite (Figure 2). Absorbencies of superabsorbent composites first increased and then decreased as the AM to AA weight ratio increased. This effect was observed in samples subjected to both distilled water and saline solution treatments. When the ratio was 200 wt%, maximum absorbencies were observed at 1516 g/g (distilled water) and 48 g/g (0.9 wt% NaCl solution), indicating a superior alternate polymer chain structure.

When AM to AA weight ratios were less than 200 wt%, absorbencies of superabsorbent composites increased with increasing AM to AA weight ratios in both distilled water and saline solution. Increasing levels of AM, a nonion group that may improve salt resistance in polymers, may be involved with this process. An increase in crosslinking was also observed between WMCAA and P(AA-co-AM) as AM levels increased, enhancing absorbency of the superabsorbent composite material in distilled water.

When AM to AA weight ratios exceeded 200 wt%, absorbencies decreased as AM increased, likely due to ionization effects. Specifically, $-\text{COONa}$ may ionize into $-\text{COO}^-$ in water, producing a hydrophilicity of $-\text{COO}^-$ superior to that of $-\text{CONH}_2$.

Effect of Initiator Content

Varying the amount of KPS initiator affected absorbency (Figure 3). Absorbencies increased with increasing KPS

concentrations from 0.3 wt% to 1.3 wt%. The maximum absorbencies of 1512 g/g (distilled water) and 47 g/g (0.9 wt% NaCl solution) were obtained at 1.3 wt% of KPS.

For KPS concentrations in excesses of 1.3 wt%, absorbencies decreased with further increases in KPS concentration, indicating that KPS concentration significantly influenced polymer absorbency. This finding is in accordance with the previously characterized relationship between average chain length and initiator concentration during polymerization.²⁶ Further increasing the initiator concentrations from 1.3 wt% to 5.3 wt% reduced absorbencies, attributable to the scarcity of radicals produced during polymerization.

As KPS initiator concentrations increased, the molecular weight of the polymer backbone decreased, corresponding to the generation of an increasing number of polymer chain ends. Because polymer chain termination is not conducive to increased water absorbency in composites, chain termination reactions increase the amount of low molecular weight network chains. In this superabsorbent composite, the effective length of network chains was short, and stretch space was limited. Cumulatively, these produce reduced water absorbency.

Effect of Crosslinker Content

The effect of crosslinker concentrations on superabsorbent composite absorbencies were observed by varying the MBA to AA ratio (Figure 4). For MBA to AA ratios of 3 wt%, the superabsorbent composite exhibited maximum absorbencies of 1548 g/g (distilled water) and 70 g/g (0.9 wt% NaCl solution).

For MBA to AA ratios less than 3 wt%, absorbencies of superabsorbent composites in distilled water or saline solution increased with the increasing MBA to AA ratios. According to Flory's network theory, the concentration of crosslinking chains is an important factor influencing crosslinking density and fluid absorbency in hydrogel materials. On the basis of this theory, increasing crosslinking may increase the number of network nodes, and thus, improve the crosslinking density. These effects are favorable to fluid absorption and retention.

For MBA to AA ratios greater than 3 wt%, absorbencies of superabsorbent composites in distilled water or saline solution decreased with increasing MBA to AA ratios. Generation of

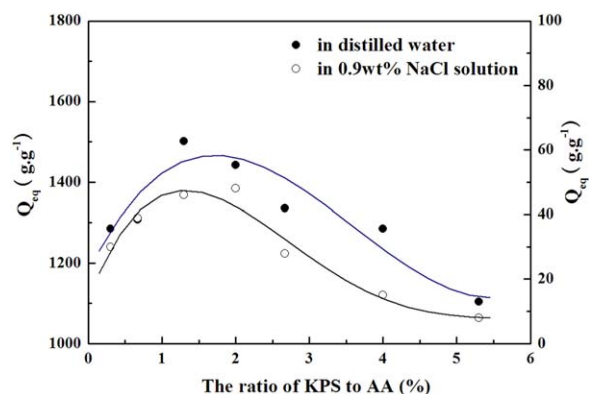


Figure 3. Effect of KPS to AA ratio on absorbencies. [Color figure can be viewed in the online issue, which is available at wileyonlinelibrary.com.]

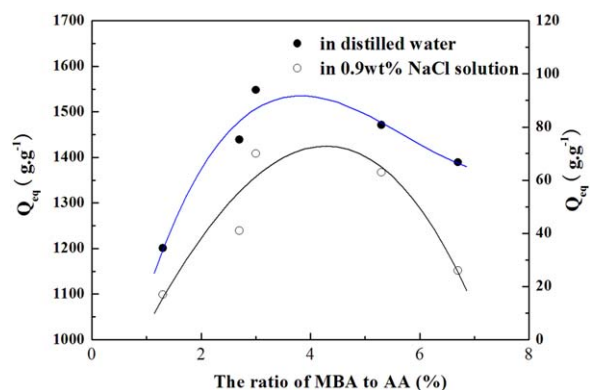


Figure 4. Effect of MBA to AA ratio on absorbencies. [Color figure can be viewed in the online issue, which is available at wileyonlinelibrary.com.]

excessive nodes in the polymeric network due to increased crosslinkers may have produced a highly crosslinked and rigid structure contributing to these observations. Hypothetically, the proposed structure would fail to expand upon fluid exposure, thus retaining little water. Thus, superabsorbent composites with moderately crosslinked hydrophilic polymer networks can absorb and retain large quantities of aqueous fluids.

Effect of AA Neutralization Degree

The ratio of different hydrophilic groups, such as $-\text{COOH}$, $-\text{COONH}_2$, and $-\text{COO}^-$, can be regulated by neutralization degree (Figure 5). Absorbencies of the composite material increased with increasing AA neutralization degree for neutralization degrees less than 75%, and decreased when AA neutralization degree was increased to 90%. Maximum absorbencies of 1123 g/g (distilled water) and 50 g/g (0.9 wt% NaCl solution) appeared at an AA neutralization degree of 75%. Accordingly, swelling capacity and absorbencies were influenced by the rubbery elasticity, ionic osmotic, and affinity of the polymer for water.²⁷

Assuming that AA is neutralized by sodium hydroxide as the number of hydrophilic groups in the composite material and osmotic pressure increase, network expansion could be observed. Therefore, increasing neutralization degree from 65 to 75% was expected to result in increasing absorbency. Experimental neutralization exceeding 75%, however, decreased

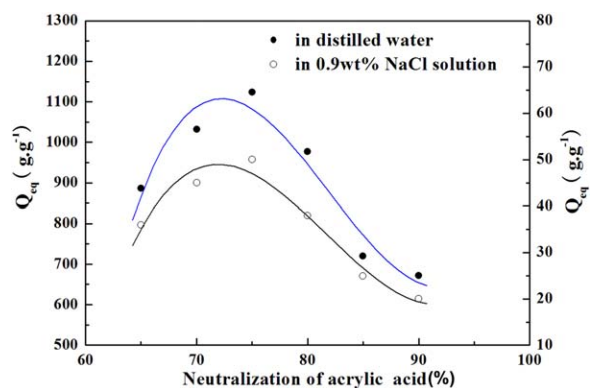


Figure 5. Effect of AA neutralization on absorbencies. [Color figure can be viewed in the online issue, which is available at wileyonlinelibrary.com.]

swelling ability. Increasing numbers of Na^+ ions in the polymeric network, leading to higher net charge density per unit chain length, may have contributed to the observed decreased swelling ability.

Infrared Spectra

The FTIR spectra of WMCAA and WMCAA/P(AA-co-AM) superabsorbent composites are shown in Figure 6. The absorption at 3414 cm^{-1} (stretching vibration of O-H), 2932 cm^{-1} (symmetrical stretching vibration of $-\text{CH}_2-$), 1454 cm^{-1} (symmetrical stretching vibration of $-\text{CH}_3$), 1322 cm^{-1} (symmetrical stretching vibration of $-\text{OH}$), and 1117 cm^{-1} and 1036 cm^{-1} (asymmetrical stretching vibrations of C-O-C) were characteristic absorptions expected from the cellulose and methylcellulose structures found in WMCAA. In addition, Figure 6(a) shows absorption bands at 898 and 1246 cm^{-1} (stretching vibration of O-glycosidic bond groups), 1375 cm^{-1} (C-H deformation vibration cellulose), 1422 cm^{-1} (combination band due to C-O stretching and O-H deformation vibration), 1509 cm^{-1} (N-H deformation vibrations), and 1650 and 1730 cm^{-1} (C=C stretching vibrations) that appeared in the spectra but disappeared following the reaction. Compared with the FTIR spectra of WMCAA and WMCAA/P(AA-co-AM), the superabsorbent composites showed new absorption bands at 1170 cm^{-1} (C-O stretching vibration), 1404 and 1562 cm^{-1} (asymmetrical stretching vibrations of $-\text{COO}-$ groups), and 1665 cm^{-1} (stretching vibration of $-\text{CON}-$). These findings cumulatively indicate copolymerization of AA and AM monomers in the presence of WMCAA, thus constructing an interpenetrated network between WMCAA and P(AA-co-AM).

Thermal Stability

TG-DTG curves of WMACC and WMCAA/P(AA-co-AM) superabsorbent composites are depicted in Figure 7. Both WMCAA and WMCAA/P(AA-co-AM) materials exhibit three-step continuous thermal decomposition. Notably, the weight-loss rate of WMCAA/P(AA-co-AM) was obviously inhibited. Weight losses of $\sim 6.4\text{ wt\%}$ ($96\text{--}196^\circ\text{C}$) for WMCAA/P(AA-co-AM) and $\sim 6.8\text{ wt\%}$ ($75\text{--}154^\circ\text{C}$) for WMCAA were observed. These values correspond to the removal of absorbed

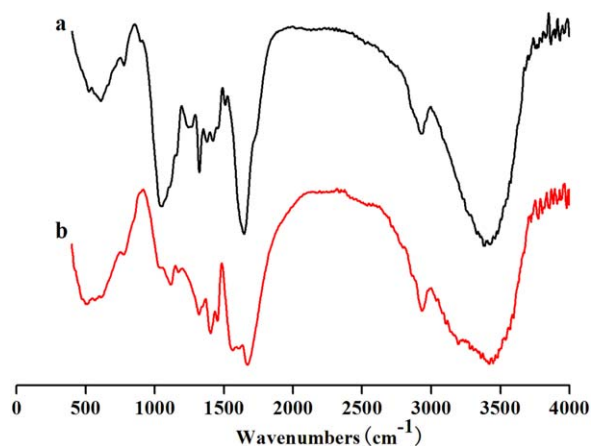


Figure 6. FTIR spectra of WMCAA (a) and WMCAA/P(AA-co-AM) (b) superabsorbent composites. [Color figure can be viewed in the online issue, which is available at wileyonlinelibrary.com.]

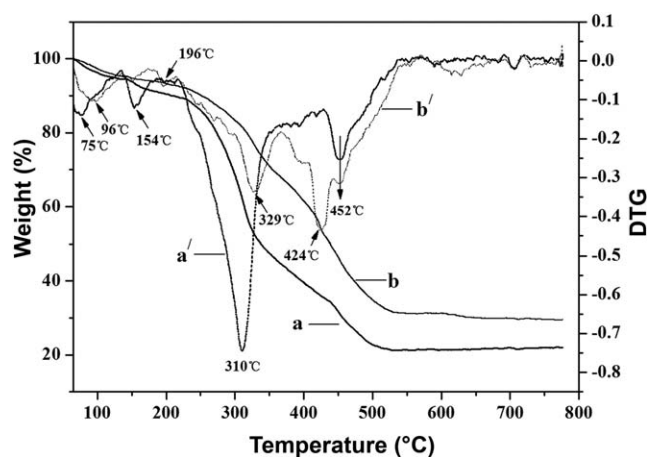


Figure 7. TG/DTG curves of WMCAA (a) and WMCAA/P(AA-co-AM) (b) superabsorbent composites.

and bonded water. Additionally, weight losses of ~ 16.8 wt% (196–329°C) for WMCAA/P(AA-co-AM) and ~ 31.5 wt% (154–310°C) for WMACC can be attributed to the dehydration of saccharide rings, breaking of C–O–C bonds in the WMACC chain, and the formation of anhydride by elimination of water molecules from neighboring carboxylic groups in grafted chains. Weight losses of ~ 12.7 wt% (329–424°C) for WMCAA/P(AA-co-AM) and ~ 31.2 wt% (310–452°C) for WMACC are potentially due to breakage of WMCAA/P(AA-co-AM) chains and subsequent deterioration of the crosslinked network structure.

DTG curves confirmed TG results. The WMCAA/P(AA-co-AM) composite hydrogel was found to be more resistant to thermal stress than WMCAA. WMACC, however, exhibited the greatest weight loss at 310°C. Weight loss peaks shifted to the high temperature region of the DTG curves, revealing delayed thermal decomposition of the hydrogel. As described previously, the WMCAA/P(AA-co-AM) composite exhibited notably slower weight loss and thermal weight loss rates. The network in this material may act as a heat barrier, enhancing overall thermal stability in the composite.²⁸

SEM, EDS, and TEM Analyses

SEM micrographs of both WMCAA and WMCAA/P(AA-co-AM) morphologies are shown in Figure 8(a,b), respectively. WMCAA has a coarse and loose surface [Figure 8(a)]. After forming the WMCAA/P(AA-co-AM) composite, the surface exhibited a smooth, compact, and porous structure [Figure 8(b)]. The porous structure contributed to aqueous fluid diffusion in the polymeric network, producing higher swelling capacity in the final hydrogel.²⁹ The smooth and compact structure suggests that WMCAA combines completely with the P(AA-co-AM) matrix, indicating homogeneous composition in the superabsorbent material.

The EDS spectrograms of WMCAA and WMCAA/P(AA-co-AM) superabsorbent composites are shown in Figure 8(c,d), respectively, and further detail is shown in Figure 8e. The characteristic peaks of C, N, O, Na, Mg, Al, Si, S, K, and Ca elements both appear in the EDS spectrogram of WMCAA and

WMCAA/P(AA-co-AM). The characteristic peaks of N, Na, and K elements in the EDS spectrogram of WMCAA/P(AA-co-AM), however, are elevated; whereas, the characteristic peaks of Mg and Ca elements in the EDS spectrogram of WMCAA/P(AA-co-AM) are lower. Copolymerization between WMCAA and acrylic acid monomers occurring with ammonium persulfate as the initiator and *N*, *N*'-methylenebisacrylamide as the cross-linker may contribute to these observations. Moreover, TEM images of the WMCAA/P(AA-co-AM) composite revealed that WMCAA platelets were well dispersed in the P(AA-co-AM) matrix, further suggesting formation of an interpenetrating polymer network structure.

Swelling Rate of the Superabsorbent Composite

Preliminary examination of the water absorption rate of the superabsorbent composite (Figure 9) produced a time course of swelling for the WMCAA/P(AA-co-AM) superabsorbent composite material. Water uptake was relatively rapid, achieving equilibrium within 20 min. Polymer absorption rates were also high. If polymer swelling exhibits first-order dynamics,³⁰ as expected, the swelling rate at a given temperature can be calculated as follows:

$$\frac{dQ_t}{dt} = k(Q_e - Q_t),$$

where t is the swelling time, Q_t is the swelling ratio at that time, and Q_e is the equilibrium swelling ratio. The equation can be integrated:

$$\begin{aligned} \int_{Q_0}^{Q_t} \frac{dQ_t}{Q_e - Q_t} &= \int_0^t k dt \\ \therefore \ln \frac{Q_e - Q_0}{Q_e - Q_t} &= kt \\ \therefore Q_t &= Q_e - \frac{Q_e - Q_0}{e^{kt}} \end{aligned}$$

The swelling rate constant (k) was obtained by plotting the equation:

$$\ln \frac{Q_e - Q_0}{Q_e - Q_t},$$

versus time (t). The theoretical swelling curve of the polymer was drawn according to the final derivation above. As shown in Figure 9, the theoretical calculations and experimental results were in close agreement, substantiating that the swelling processes adhered to first-order dynamics.

Water Absorption and Adsorption Properties of Superabsorbent Composites in Fertilizers

Fertilizer adsorptions and water absorbencies of superabsorbent composites in four fertilizer solutions are shown in Table I, showing significantly reduced water absorption rates of the WMCAA/P(AA-co-AM) composite that increased with increasing fertilizer concentrations for all fertilizer solutions.

Urea exerted minimal influence on water absorption rates. For fertilizer concentration of 5 g/L, water absorption rates in CO(NH₂)₂, NH₄Cl, KH₂PO₄, and KCl solutions were reduced to 24.79%, 81.19%, 91.44%, and 86.84% relative to those observed in distilled water, likely due to the difference between

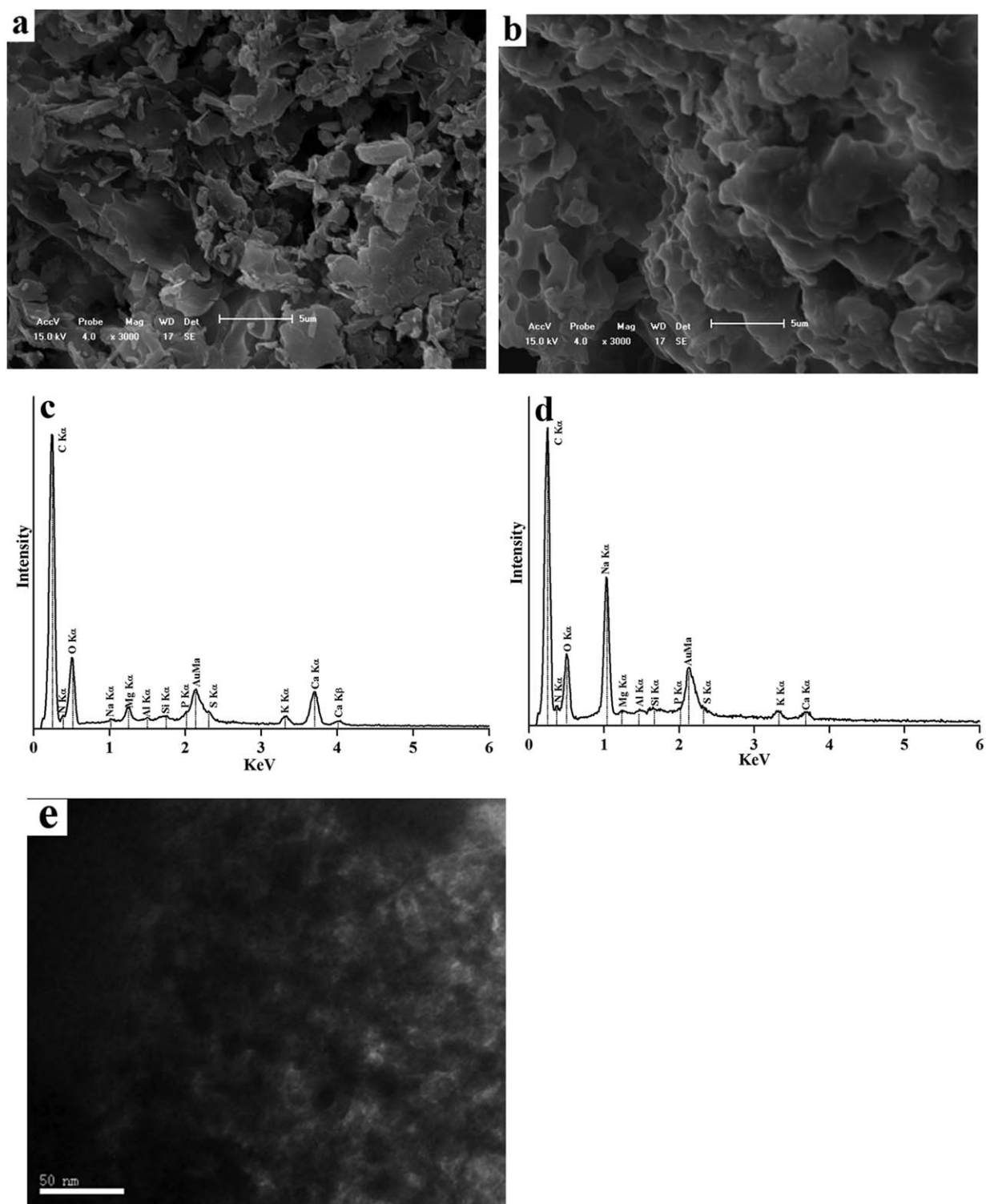


Figure 8. SEM of WMCAA (a) and WMCAA/P(AA-co-AM) (b) superabsorbent composites; EDS curves of WMCAA (c) and WMCAA/P(AA-co-AM) (d) superabsorbent composites; and TEM of WMCAA/P(AA-co-AM) (e) superabsorbent composites.

urea and the other three electrolyte fertilizers. Notably, urea is a nonelectrolyte that exists in the molecular, non-ionized form in aqueous solution. Thus, preparation of superabsorbent resins inherently involves a certain degree of electrolyte crosslinking,

producing a crosslinked network containing many hydrophilic groups, including $-\text{COO}^-$ and $-\text{OH}$. The existence of osmotic pressure differentials in superabsorbent resin solutions may cause water molecules to move in the direction of the electrolyte

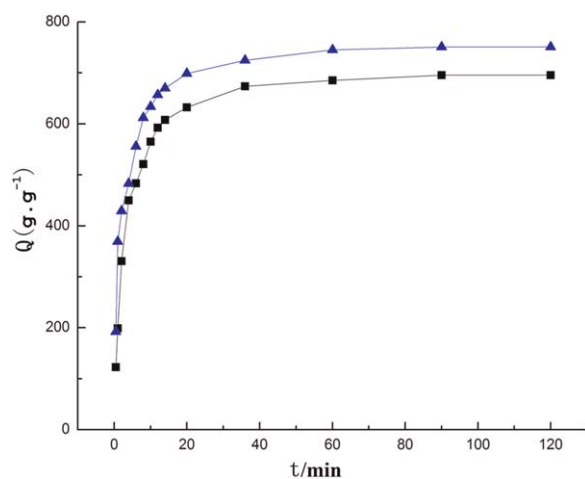


Figure 9. The time course of water absorption for superabsorbent composite samples. The square and triangle symbols represent experimental data; solid lines represent theoretical calculations. [Color figure can be viewed in the online issue, which is available at wileyonlinelibrary.com.]

dilution concentration. Thus, urea-based fertilizers are less likely to be affected by the water absorbing capacity of superabsorbent resins.

In the 20 g/L urea solution, the relative water absorbency of superabsorbent composite was still observed to be as high as 69.25%; however, in solutions with identical concentrations of NH_4Cl , KH_2PO_4 , or KCl , the relative water absorbency of the superabsorbent composite was found to be less than 9%. This discrepancy between fertilizer types demonstrates that the influence on water absorption ratios in electrolyte-based fertilizers was significantly larger. According to the Flory gel swelling formula:

$$Q^{\frac{5}{3}} \approx \frac{\left(\frac{i}{2V_u S^2}\right)^2 + \frac{\frac{1}{2} - \chi_1}{V_1}}{\frac{V_e}{V_0}},$$

where Q is the water absorption ratio, S is the external solvent ionic strength, i/V_u is the polymer charge density, χ_1 is the interaction parameter, V_1 is the polymer than volume, and V_e/V_0 is the polymer crosslinking density. The first section of the equation represents the molecular part of osmotic pressure. The greater the ionic strength, the smaller is the osmotic pressure in the solution. Thus, smaller water absorption ratios result as in the experimental study.

The ionic strengths of NH_4Cl , KH_2PO_4 , and KCl solutions was higher than the ionic strength of the urea solution, dramatically reducing water absorption ratios for superabsorbent resins treated with these fertilizers. Furthermore, superabsorbent polymers exhibit distinct adsorption capacities for each of the four fertilizer solution types (Table I). The largest and smallest adsorption amounts were observed for urea and KH_2PO_4 , respectively.

Also, the amount of water retention agent (superabsorbent composite) adsorbed in each fertilizer increased with increasing fertilizer solution concentration. Within a certain range, higher

Table I. Relative Water Absorbency Rate and Adsorption Quantity of Superabsorbent Resin in Different Fertilizer Solutions

	$\text{CO}(\text{NH}_2)_2$ (g/L)			NH_4Cl (g/L)			KH_2PO_4 (g/L)			KCl (g/L)						
	0	5	10	5	10	20	5	10	20	5	10	20				
Relative water absorbency (%)	100	75.21	72.14	69.25	100	18.81	15.23	8.05	100	8.56	3.89	2.01	100	13.16	10.51	6.63
Relative amount of adsorption (g/g)	0	3.82	8.58	14.67	0	2.32	2.66	3.41	0	1.21	1.85	2.07	0	1.82	3.05	4.38

fertilizer concentrations indicated greater adsorption. Under identical concentration conditions, urea adsorption of superabsorbent resin was always higher than NH_4Cl or KH_2PO_4 adsorption of superabsorbent resin, which was extremely low in both cases. Therefore, urea is more suitable for nitrogen and water retention agent collection than NH_4Cl . Additionally, adsorption of superabsorbent resin in KCl was superior to that observed in KH_2PO_4 .

CONCLUSIONS

A novel superabsorbent composite was synthesized by graft copolymerization using acrylic acid (AA) and acrylamide (AM) coupled with naturally occurring waste material cultured *Auricularia auricula* (WMCAA) in aqueous solution initiated by microwave irradiation. This highly efficient synthesis method can also reduce the production of harmful environmental pollutants produced by conventional synthesis methods, allowing for cleaner commercial production. Additionally, this method is economical for superabsorbent polymer composites production, enabling utilization of existing WMCSS bioresources prevalent in China. Notably, WMCAA is susceptible to degradation by bacteria and other microorganisms due to its rich nutrient content (N, P, K, and other trace elements). The proposed superabsorbent composite material exhibited a maximum water absorbency of 1548 g/g in distilled water and 72 g/g in 0.9% NaCl, and it demonstrated superior water absorption and adsorption properties when exposed to urea-based fertilizer solutions. Therefore, these superabsorbent composites may be widely applicable as an alternative for enhancing water irrigation and fertilizer utilization in commercial agriculture and forestry industries.

REFERENCES

1. Dubrovskii, S.; Afanas'eva, M.; Lagutina, M.; Kazanskii, K. *Polym. Bull.* **1990**, *24*, 107.
2. Bajpai, S.; Johnson, S. *React. Funct. Polym.* **2005**, *62*, 271.
3. Pourjavadi, A.; Ayyari, M.; Amini-Fazl, M. *Eur. Polym. J.* **2008**, *44*, 1209.
4. Chen, J.; Park, K. *J. Control. Release* **2000**, *65*, 73.
5. Ma, F.; Song, L.; Duo, Y.; Liao, S.; Tan, H. *Polym. Mater. Sci. Eng.* **2003**, *19*, 81.
6. Das, A.; Kothari, V.; Makhija, S.; Avyaya, K. *J. Appl. Polym. Sci.* **2007**, *107*, 1466.
7. Teodorescu, M.; Lungu, A.; Stanescu, P. O. *Indus. Eng. Chem. Res.* **2009**, *48*, 6527.
8. Guilherme, M. R.; Reis, A. V.; Paulino, A. T.; Moia, T. A.; Mattoso, L. H. C.; Tambourgi, E. B. *J. Appl. Polym. Sci.* **2010**, *117*, 3146.
9. Kandile, N. G.; Nasr, A. S. *Carbohydr. Polym.* **2009**, *78*, 753.
10. Sadeghi, M.; Hosseinzadeh, H. *J. Bioact. Compat. Polym.* **2008**, *23*, 381.
11. Pourjavadi, A.; Barzegar, S. *Starch-Stärke* **2009**, *61*, 161.
12. Cheung, H. Y.; Lau, K. T.; Lu, T. P.; Hui, D. *Compos. Part B: Eng.* **2007**, *38*, 291.
13. Yang, L.; Ma, X.; Guo, N. *Carbohydr. Polym.* **2011**, *85*, 413.
14. Yoshimura, T.; Uchikoshi, I.; Yoshiura, Y.; Fujioka, R. *Carbohydr. Polym.* **2005**, *61*, 322.
15. Tao, M.; Jiao, X. *J. China Agri. Univ.* **2009**, *14*, 118.
16. Shao, J.; Yang, Y.; Zhong, Q. *Polym. Degrad. Stabil.* **2003**, *82*, 395.
17. Xu, K.; Song, C.; Zhang, W.; Luo, Y.; Dong, L.; Wang, P. *J. Funct. Polym.* **2004**, *17*, 473.
18. Tong, Z.; Peng, W.; Zhiqian, Z.; Baoxiu, Z. *J. Appl. Polym. Sci.* **2004**, *95*, 264.
19. Singh, V.; Tripathi, D. N.; Tiwari, A.; Sanghi, R. *J. Appl. Polym. Sci.* **2004**, *95*, 820.
20. Wang, P. *Environmental Microwave Chemistry Technology*; Chemical Industry Press: Beijing, **2003**.
21. Hou, L.; Yao, F.; Gao, R.; Chen, Y. *Ed. Fungi China* **2008**, *3*, 004.
22. Zhou, F. *Soil Fert.* **1991**, *25*, 42.
23. Zheng, L. Y.; Huang, X. Q.; Peng, W. H. *Acta Edulis. Fungi* **2006**, *13*, 76.
24. Li, X. M. *J. Henan Agricultural Sciences China* **2003**, *5*, 40.
25. Xie, X. H.; Liang, Y. J.; Li, Y. J. *Soil Water Conserv.* **2008**, *22*
26. Zhang, J. P.; Wang, Q.; Wang, A. Q. *Carbohydr. Polym.* **2007**, *68*, 367.
27. Pourjavadi, A.; Amini-Fazl, M. S. *Polym. Int.* **2006**, *56*, 283.
28. Liu, Z.; Miao, Y.; Wang, Z.; Yin, G. *Carbohydr. Polym.* **2009**, *77*, 131.
29. Santiago, F.; Mucientes, A. E.; Osorio, M.; Rivera, C. *Eur. Polym. J.* **2007**, *43*, 1–9.
30. Liu, M.; Cheng, R.; Qian, R. *Acta Polym. Sin.* **1996**, *2*, 234.